Engineering Computations

Evidential uncertainty quantification of the Park-Ang damage model in performance based design

Hesheng Tang, Dawei Li, Lixin Deng, Songtao Xue,

Received 26 November 2017
Revised 28 April 2018
14 June 2018
Accepted 27 June 2018

Evidential uncertainty quantification of the Park–Ang damage model in performance based design

Hesheng Tang
State Key Laboratory for Disaster Reduction in Civil Engineering, Tongji University, Shanghai, China and Research Institute of Structural Engineering and Disaster Reduction, Tongji University, Shanghai, China, and

Dawei Li, Lixin Deng and Songtao Xue
Research Institute of Structural Engineering and Disaster Reduction, Tongji University, Shanghai, China

Abstract

Purpose – This paper aims to develop a comprehensive uncertainty quantification method using evidence theory for Park–Ang damage index-based performance design in which epistemic uncertainties are considered. Various sources of uncertainty emanating from the database of the cyclic test results of RC members provided by the Pacific Earthquake Engineering Research Center are taken into account.

Design/methodology/approach – In this paper, an uncertainty quantification methodology based on evidence theory is presented for the whole process of performance-based seismic design (PBSD), while considering uncertainty in the Park–Ang damage model. To alleviate the burden of high computational cost in propagating uncertainty, the differential evolution interval optimization strategy is used for efficiently finding the propagated belief structure throughout the whole design process.

Findings – The investigation results of this paper demonstrate that the uncertainty rooted in Park–Ang damage model have a significant influence on PBSD design and evaluation. It might be worth noting that the epistemic uncertainty present in the Park–Ang damage model needs to be considered to avoid underestimating the true uncertainty.

Originality/value – This paper presents an evidence theory-based uncertainty quantification framework for the whole process of PBSD.

Keywords Differential evolution algorithm, Epistemic uncertainty, Evidence theory, Park-Ang damage model, Performance-based seismic design

Paper type Research paper

1. Introduction

There is increasing agreements that performance-based earthquake engineering will be the next-generation seismic design and evaluation framework (SEAOC Vision 2000, 1995). Some far-reaching guidelines for seismic design (FEMA356, 2000) are also credited with laying the foundation for the performance-based seismic design (PBSD) concept. As the crucial roadmap for prospective PBSD approach, the SEAOC Vision 2000 (1995) documented such

This study was supported by the Ministry of Science and Technology of China, Grant No. SLDRCE14-B-03 and the National Natural Science Foundation of China, Grant No. 51178337.

Engineering Computations
Vol. 35 No. 7, 2018
pp. 2480-2501

0264-4401
DOI 10.1108/EC-11-2017-0466

potential performance indicators which involves in displacement-based design, energy-based design and comprehensive design considering lifecycle cost, respectively. Among these three potentials, the displacement-based design approach is the most commonly implemented, due to its concise performance indicator (e.g. inelastic displacement, maximum inter story drift ratio, ductility demand, etc.). (Chopra and Goel, 1999; Priestley *et al.*, 2007). Although a displacement-based approach is more sophisticated than force-based methods for describing structural damage, the introduction of energy dissipation makes the quantification of seismic structural damage more reasonable (Ghosh and Collins, 2006; Datta and Ghosh, 2008). This is because the simple measures of displacement or ductility demand may not fully capture the main characteristic behavior of high inelastic excursions under loading directions. Dissipated energy is a cumulative parameter involving cyclic–plastic deformation in a structure during earthquakes and is more appropriate to evaluate the seismic demand for an inelastic system than a non-cumulative index. However, a large scale of laboratory experiments manifest that the excessive deformation and hysteretic energy are both contributing to seismic damage of structural component. Hence, the damage models combining deformation ductility and hysteretic energy appear to be more reasonable. One of the most acceptable damage indices is the Park–Ang damage index proposed by Park and Ang in 1985 (Park and Ang, 1985), which takes into account the effects of both displacement ductility demand and hysteretic energy demand in low-cycle-fatigue for a structural component during cyclic load. Due to the intrinsic simplicity as well as a significant amount of experimental foundations, the Park–Ang and other similar damage indices have been widely used in damage-based seismic design (Park *et al.*, 1987; OU *et al.*, 1999; Hajirasouliha *et al.*, 2012) and performance evaluation of structures (Park *et al.*, 1985; Williams and Sexsmith, 1997; Zhai *et al.*, 2013; Karbassi *et al.*, 2014).

Although, the effectiveness of using the Park–Ang model and its modified versions has been supported by many researchers, it should be noted that Park–Ang damage index-based seismic design and evaluation is a very challenging task due to the large uncertainties associated with this damage model. The high level of uncertainties in the Park–Ang damage model result from the assumption of damage model formulation and related parameter calibration using limited experimental data (Kunnath *et al.*, 1990; Rajabi *et al.*, 2013; Park and Ang, 1985). Based on this, the significant variability observed in the cyclic test results of RC structural members requires the application of uncertainty modeling techniques for PBSD analysis. Moreover, both sources of uncertainty, which arise inevitably in this analysis and assessment process, are equally important and must be considered in the design and evaluation. Hence, it is necessary to present a comprehensive seismic performance assessment methodology to quantify the uncertainties and obtain more reliable results.

According to the nature of uncertainties, the uncertainties can be classified as aleatory and epistemic. The aleatory uncertainty (Oberkampf *et al.*, 2001; Helton, 1997) can be well quantified by probability theory, which mainly relies on either abundant or relatively complete statistical information for the probabilistic uncertainty description. However, classical probability theory is not appropriate for epistemic uncertainty owing to the lack of knowledge or information (Oberkampf *et al.*, 2001; Helton, 1997). In the past decades, several alternative approaches for dealing with epistemic uncertainty have been developed, such as fuzzy sets theory (Zadeh, 1965), interval analysis (Moore, 1966), possibility theory (Dubois and Prade, 1988), imprecise probability theory (Walley, 1991) and evidence theory (Dempster, 1967; Shafer, 1976). With flexibility of theoretical body, evidence theory allows the combination of aleatory and epistemic uncertainty in a straightforward way without any assumptions. This great potential is more general than probability and possibility theories (Klir and Smith, 2001).

In recent years, evidence theory methods have developed rapidly, providing a solid theoretical basis for epistemic uncertainty quantification (UQ) (Bae *et al.*, 2004; Salehghaffari *et al.*, 2012), risk assessment (Lo *et al.*, 2014) and reliability analysis (Sallak *et al.*, 2013). As reflected in the aforementioned work, some inspiring progresses have been made for evidence theory-based uncertainty modeling. However, it still not be extensively used in large and complex engineering due to the computational intensiveness problem. As the result of the direct representation of uncertainty with many discrete sets, the evidential uncertainty propagation needs the evaluation of the bound values over all possible sets. Thus, the huge time-cost consuming is inevitable. To alleviate the computational difficulties in the evidence theory-based UQ analysis, the principle and method of using differential evolution-based interval optimization are introduced to enhance the computational efficiency as described previously by the authors (Tang *et al.*, 2015).

Considering the strong capabilities of evidence theory for tackling with epistemic uncertainties with its flexible methodology of construction of basic belief assignment (BBA) and reasonable measures using belief and plausibility functions to measure the likelihood of events, this paper develops an UQ method using evidence theory for Park–Ang damage index-based performance design in which epistemic uncertainties are considered. This article is organized as follows. The description of the Park–Ang damage model-based PBSD and the associated sources of uncertainties are presented in Section 2. Uncertainties emanating from the experimental results of RC members provided by the Pacific Earthquake Engineering Research Center are addressed herein. A methodology of evidence theory-based UQ for the Park–Ang model based PBSD is briefly described in Section 3. For investigating the capability of the proposed methodology and the influence of the uncertainties rooted in the Park–Ang damage model, a comparison between the analysis results of evidence theory and a probabilistic method for PBSD of a multi-story RC structure is performed in Section 4. Conclusions are provided in Section 5.

2. Sources of uncertainty in the Park–Ang damage index based performance-based seismic design

2.1 The Park–Ang damage index-based performance-based seismic design

The Park–Ang damage model (Park and Ang, 1985), combining excessive displacement and cumulative hysteretic energy, used to evaluate the structural damage state is defined as:

$$D = \frac{\delta_{\mathrm{m}}}{\delta_{\mathrm{u}}} + \beta \frac{E_{\mathrm{h}}}{Q_{\mathrm{y}}\delta_{\mathrm{u}}} \qquad (1)$$

where D is the damage index; δ_{m} is the maximum deformation under cycle loading; δ_{u} is the ultimate deformation under monotonic loading; E_{h} is the dissipated hysteretic energy; Q_{y} is the yield strength; and β is the combine parameter. Referring to previous studies, the performance seismic design-based Park–Ang damage model involves two important parallels. One synthesizes a preliminary design based on building design codes and damage assessment for structural elements or an entire building, but it should be noted that this process involves a series of time history dynamic analyses to validate the damage state of the structure. Alternatively, the other directly applies the damage model to estimate the structural elemental or entire seismic performance demand, while avoiding the repeated iterations for the validation process on the damage state. For the objective of being concise, we chose the latter design process to clarify the uncertainty influence rooted in the Park–Ang model for PBSD.

In the preceding investigation for the damage state of an equivalent single degree of freedom system (ESDOF), Fajfar (1992) introduced factors $\mu_{\mathrm{m}} = \delta_{\mathrm{m}}/\delta_y$ and $\mu_u = \delta_u/\delta_y$ to denote the maximum ductility of the ESDOF under cyclic and monotonic loading, respectively. Substituting these two factors into equation (1) leads to:

$$D = \frac{\mu_{\mathrm{m}}}{\mu_{\mathrm{u}}} + \beta \frac{E_{\mathrm{h}}}{Q_{\mathrm{y}}\mu_{\mathrm{u}}\delta_y} \tag{2}$$

Using a dimensionless constant $\gamma = \sqrt{\mathrm{E_h/F_y}\ \delta_{\mathrm{y}}}/\ \mu_{\mathrm{m}}$ with equation (2), the demand ductility factor μ can be evaluated by the designated damage index D:

$$\mu = \left(\sqrt{1 + 4\beta D\gamma^2\mu_{\mathrm{u}}} - 1\right)/2\beta\,\gamma^2 \tag{3}$$

Based on the hypothesis that the damage state of each vertical element is uniform in an arbitrary floor for a regular low-rise structure, Zhang *et al.* (2011) argued that the *i*th-floor ductility factor of structure $\overline{\mu_i}$ is developed using the following:

$$\overline{\mu_i} = \mu_{ij} = \left(\sqrt{1 + 4\beta_{ij}D_{ij}\gamma_{ij}^2\mu_{\mathrm{u},ij}} - 1\right)/2\beta_{ij}\gamma_{ij}^2 \tag{4}$$

where μ_{ij} is the demand ductility factor for the *j*th vertical element of the *i*th floor, and other factors related to *i* and *j* have analogous meanings. From the above derivation, the demand ductility factor of an arbitrary floor μ_i can be calculated by the established D_{ij}, β_{ij}, $\mu_{u,ij}$ and γ_{ij}.

On the other hand, relying on Chorp's (Chopra and Goel, 1999) assumption of the transformational relation between multi degree of freedom systems and ESDOFs, the *i*th-floor maximum inter-story displacement $\delta_{\mathrm{m},i}$ and the *i*th-floor yield inter-story of the fundamental mode $\delta_{\mathrm{y},i}$ are respectively represented as:

$$\delta_{\mathrm{m},i} = \Gamma_1 q_{\mathrm{m}}(\Phi_{1,i} - \Phi_{1,i-1}) \tag{5}$$

$$\delta_{\mathrm{y},i} = \Gamma_1 q_{\mathrm{y}}(\Phi_{1,i} - \Phi_{1,i-1}) \tag{6}$$

where $\Phi_{1,i}$ is the *i*th element of the fundamental mode; $\Phi_{1,i-1}$ is the $i-1$th element of the fundamental mode, q_{m} is the maximum drift for an ESDOF; q_{y} is the yield drift for an ESDOF; and Γ_1 is the fundamental mode participation factor. Dividing equation (5) by equation (6), the relation of the demand ductility factor $\overline{\mu_i}$ for the *i*th floor and μ_{eq} for an ESDOF follows:

$$\overline{\mu_i} = q_{\mathrm{m}}/q_{\mathrm{y}} = \mu_{\mathrm{eq}} \tag{7}$$

Substituting equation (4) into this expression, gives:

$$\mu_{\mathrm{eq}} = \left(\sqrt{1 + 4\beta_{ij}D_{ij}\gamma_{ij}^2\mu_{\mathrm{u},ij}} - 1\right)/2\beta_{ij}\gamma_{ij}^2 \tag{8}$$

With the purpose of detailed structural design, the seismic ductility demand should be transformed into the strength demand through the relationship of R–μ–T that has been proposed by many researchers (Miranda, 1993; Vidic *et al.*, 1994; Zhuo and Fan, 2001). In this paper, the empirical formula presented by Zhuo and Fan (2001) with the site classification of the Chinese seismic code (GB50011-2010, 2010) is adopted:

$$R(T,\mu) = 1 + (\mu - 1)(1 - e^{-AT}) + \frac{\mu - 1}{B} T \cdot e^{-CT} \tag{9}$$

where R is the strength reduction factor and T is the natural vibration period of an ESDOF, the parameter A, B and C are estimated by regression analysis and corresponding value are listed in Table I for the different classification of site.

Therefore, the strength demand of an ESDOF is determined:

$$F_{\mathrm{y}} = F_{\mathrm{E}}/R\left[\mu\left(D_{ij}, \beta_{ij}, \gamma_{ij}, \mu_{\mathrm{u},ij}\right), T\right] \tag{10}$$

where F_{E} is the elastic resistant seismic force under a major earthquake, and F_y is the yield resistant force under a major earthquake. From the formulation of equation (10), the seismic strength demand of an ESDOF is determined by F_{E}, T, D_{ij}, β_{ij}, γ_{ij} and $\mu_{\mathrm{u},ij}$. In equation (10), D_{ij} is a predetermined value, F_{E} is computed by the elastic analysis for an ESDOF under a major earthquake and T is calculated by finite element analysis in the preliminary design. The other three parameters should be assigned by theoretical studies or empirical techniques, where different researchers has presented various opinions for these parameters. The combine parameter β has been considered as 0.05 (Park *et al.*, 1987), 0.15 (Park *et al.*, 1984) or 0.24 (Alarcón *et al.*, 2001) or fitted to a set of experimental data (Kunnath *et al.*, 1990; Rajabi *et al.*, 2013). The energy parameter γ is estimated by a series of time history analyses for an SDOF (Fajfar, 1992) or the relationship of force and displacement for structural components (Rodriguez and Padilla, 2009). With regard to μ_{u}, the value is given by expert judgement or experimental measurement from component experiments (Park and Ang, 1985; Kunnath *et al.*, 1990; Panagiotakos and Fardis, 2001; Jiang *et al.*, 2010). Correspondingly, these variant choices for parameters may play a significant role in the expression of F_{y} in equation (10) and dramatically affect the results of a damage assessment and the subsequent elemental design (Ghosh *et al.*, 2011). On account of the above, the significant variability of parameters related to the Park–Ang damage model for PBSD requires the application of uncertainty modeling techniques to the PBSD analyses.

2.2 Uncertainties in the Park–Ang damage model

To illustrate the uncertainties associated with the Park–Ang damage model for PBSD, the replicate experimental results of the PEER column database compiled at the University of Washington (University of Washington, 2004) are used here. The selection criteria of calibration database is as follows:

- the cross-section of specimen is rectangular and the specimen should experience more than two hysteretic cycles;
- the failure of the specimen is classified as flexural type; and
- the longitude bars in column should not be spliced and the placement should be symmetric.

Table I.
Value of regression parameter of R–μ–T

Site classification	A	B	C
I	4.84	$0.80 + 0.89\mu$	0.4
II	3.95	$0.76 + 0.09\mu - 0.03\mu^2$	0.65
III	1.38	$0.41 + 0.06\mu - 0.003\mu^2$	0.87

Following the above three rules, the main properties: the yield stress of longitudinal reinforcement f_y, the compressive strength of concrete f_c; the axial stress ratio n_0; the shear-span λ; the confinement ratio ρ_w and the longitudinal reinforcement ratio ρ_0 of this calibrating database consists of 98 RC column tests shown in Figure 1.

As shown in Figure 1, the diverse and wide range of each main properties denote to the well covering of the specimens in the selected database. For the original Park–Ang damage model used in this work, the following empirical formula (Kunnath *et al.*, 1990) is used to calculate the value of β, and the results are shown in Figure 2(a):

$$\beta = \left[0.37n_0 + 0.36(\kappa_\rho - 0.2)^2\right] \times 0.9^{\rho_w} \tag{11}$$

where $\kappa_\rho = p_t f_y/(0.85 f_c)$; κ_ρ is the normalized longitudinal reinforcement ratio; ρ_t is the tension reinforcement ratio which always be the half of the longitudinal reinforcement ratio ρ_0 of symmetric reinforcement. Specimens in this database fail under cyclic loading, whereas the data for the ultimate response deformation of columns under monotonic loading are missing. To overcome this defect, we use the relationship of ultimate deformation under monotonic load δ_u and the ultimate deformation under cyclic load δ_{cu} (FIP, 2003) to approximate the ultimate displacement of monotonic loading. Then, the ultimate ductility factor is given by:

$$\mu_u = \frac{\delta_u}{\delta_y} = \frac{\delta_{cu}}{0.62\delta_y} \tag{12}$$

where δ_u is the ultimate response deformation under monotonic loading; δ_y is the yield response deformation under cyclic loading, which is calculated by the definition of

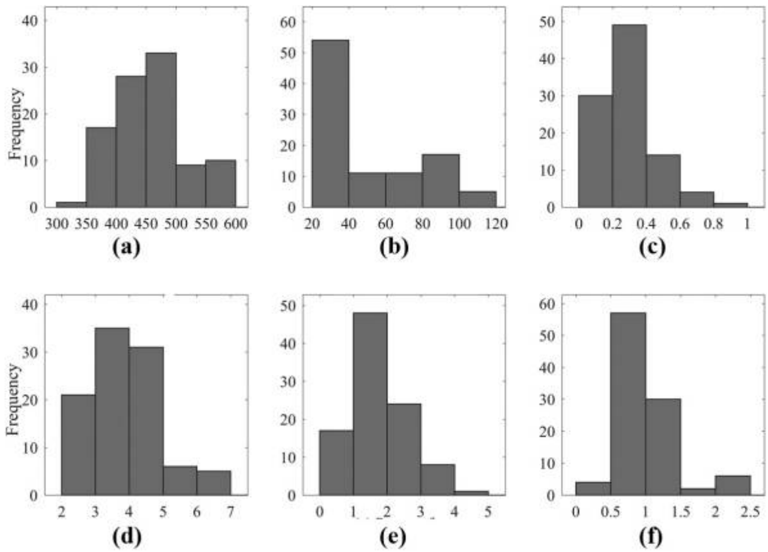

Notes: (a) Range of f_y (MPa); (b) range of f_c (MPa); (c) Range of n_0; (d) Range of λ (e) Range of p_w; (f) Range of p_0

Figure 1. The range of main properties of the calibrating database

Park (1988); δ_{cu} is the point in the slope of the envelope curve with an 85 per cent maximum strength or the point of failure of the structural component. The value of the regularized dissipated hysteretic energy parameter γ can be directly computed from:

$$\gamma = \sqrt{\frac{E_h \delta_y}{F_y \delta_m^2}} \tag{13}$$

in equation (13), E_h is the area of the complete drift curve, and F_y is the yield force of the component under cyclic loading, defined by Park (1988). From the above deduction, it can be found that these three parameters are dimensionless, and they can easily use the structural designing process.

Figure 2 shows the dimensionless model constants(β, μ_u, γ) that were evaluated from the abovementioned empirical formulas using the test data of 98 RC column sets. A wide variation in constants is shown in this figure, as expected. This variability in the calculated model constants is mainly because of the uncertainties from material properties, experimental procedure and the lack of knowledge about the physical mechanisms, etc. As the Park–Ang damage model is crucial for relating structural response in PBSD analysis of structures, any uncertainty in this model can propagate into high level of variability in the structural seismic demand and capacity predictions and affect the reliability and safety of the designed system. Therefore, it is crucial to establish a mathematical framework for UQ of the Park–Ang damage models. In the context of the UQ of performance based design and damage estimation, probability theory has been widely used to model the uncertain variable (Azhdary and Shabakhty, 2011). As we know, the probabilistic model is supported by sufficient statistical information. However, this is often not the case in Park–Ang damage based PBSD due to the limited available data and lack of knowledge about the damage mechanics. Hence, based on the nature of uncertainty in the Park–Ang damage models and the capabilities of evidence theory, we adopted this theory instead of a probabilistic method for uncertainty modeling of the Park–Ang damage models in the PBSD analysis of structures.

3. Evidence theory-based uncertainty quantification of the Park–Ang damage index based performance design

As noted in above section, the evidence theory is used here to model the epistemic uncertainties rooted in Park–Ang damage index-based performance design. To formulate

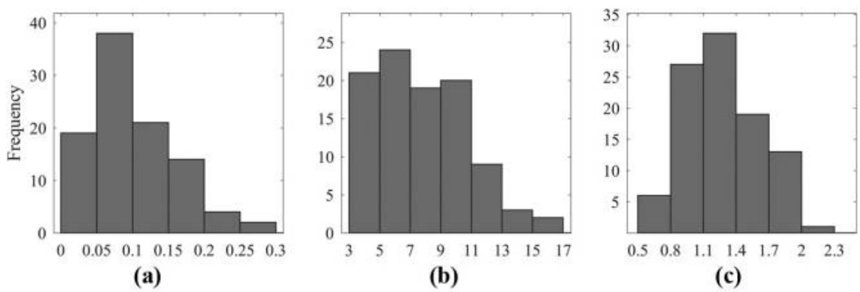

Notes: (a) Range of β; (b) range of μ_u; (c) range of γ

Figure 2. Histogram of parameters β, μ_u, γ

the UQ for PBSD systematically, the three stages, including the uncertainty representation, propagation and measurement, are briefly described.

3.1 Evidence-based uncertainty representation

The uncertainty representation, projecting the original statistical information to a specific form that can be modeled by uncertainty theory, is one of the essential procedures of UQ for the Park–Ang model-based PBSD. Using the mathematical definition of evidence theory in documents (Dempster, 1967; Shafer, 1976), the evidential representation of uncertain parameters x in Park–Ang damage model is given as:

$$x : \left\{ \left(x_1^{\mathrm{I}}, m_1 \right), \cdots, \left(x_k^{\mathrm{I}}, m_k \right), \cdots, \left(x_K^{\mathrm{I}}, m_K \right) \right\} \tag{14}$$

where $x_k^{\mathrm{I}} = [\underline{x}_k, \overline{x}_k]$ denote the kth focal element of uncertain parameter x; $\underline{x}_k$ and $\overline{x}_k$ denote the lower and upper bounds of x_k^{I}, respectively; m_k denotes the BBA of the kth focal element of uncertain parameter x. In evidence theory, the frame of discernment Θ is defined as the collection of focal elements x_k^{I}. The power set $\Omega = 2^{\Theta}$, which contains all possible subset of Θ. The focal element x_k^{I} is meaningful on the condition that $x_k^{\mathrm{I}} \subset \Omega$ and $x_k^{\mathrm{I}} \in \Theta$. The BBA of focal element x_k^{I} satisfies the following axioms:

$$\sum_{k=1}^{K} m_k = 1, \quad m_k \geq 0 \tag{15}$$

In this work, we adopt a general methodology, as described previously by Salehghaffari *et al.* (2012), to construct the evidential expression of the uncertain variables using available data. By following the idea of this methodology, the data of uncertain parameters in Park–Ang damage model is collected with histogram, and then, the uncertain information of these parameters are represented with a set of interval forms and statistical frequency, accordingly. After that, a belief structure with an assigned degree of belief for each model constant from the generated histogram by the rules of agreement, conflict and ignorance relationships in the data is constructed. This is illustrated by the example in Figure 3, which assumes that C_i denotes the number of data points included in each bin I_i and that C_{t} denotes the total number of data points in the histogram.

As indicated in Figure 3, agreement is used to represent the relationship of I_2 and I_3 by $C_2/C_3 > 0.8$, ignorance is used to indicate the relationship of I_1 and I_2 by $C_1/C_2 < 0.5$. In addition to the above two situations, the third situation is conflict (see I_3 and I_4 in Figure 3).

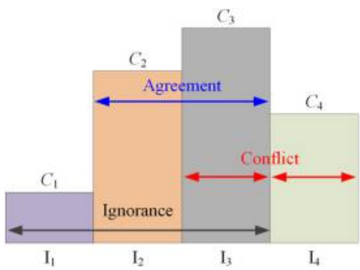

Figure 3.
Relationship of adjacent bins

According to this criterion, the reciprocal relationship of adjacent bins is constructed, and the corresponding BBA of intervals in Figure 3 are formulated as:

$$\begin{aligned} m(\{\mathrm{I}_1, \mathrm{I}_2, \mathrm{I}_3\}) &= C_1/C_\mathrm{t} \\ m(\{\mathrm{I}_2, \mathrm{I}_3\}) &= (C_2 + C_3)/C_\mathrm{t} \\ m(\{\mathrm{I}_4\}) &= C_4/C_\mathrm{t} \end{aligned} \tag{16}$$

Repeating the above two steps, the belief structure for each element of uncertain input is constructed, and additional details of evidential uncertainty representation for available data can be found in Salehghaffari *et al.* (2012).

3.2 Evidential uncertainty propagation of performance-based seismic design using differential evolution

Uncertainty propagation step is implemented here for determination of the system response of interest that is influenced by the underlying model uncertainties. To illustrate the procedure of uncertainty propagation of the Park–Ang damage index-based PBSD, we use Figure 4 (only one uncertain variable is considered): where x_i is the uncertain input, d is the deterministic input and f () is the system function designated as the framework of PBSD in this work. With the discussion in Section 2, the fundamental natural frequency T and elastic resistant seismic force F_E for ESDOF under rare earthquakes are given, and the system function related to equation (10) is specified as:

$$R(\mu, T) = R\left\{\left(\sqrt{1 + 4\beta D \gamma^2 \mu_\mathrm{u}} - 1\right)/2\beta\,\gamma^2, T\right\} \tag{17}$$

Using the evidence theory to represent the uncertain parameter β, μ_u, γ in Park–Ang damage model, the uncertain information of these parameters are represented by a set of discrete intervals. Thus, the joint uncertain system input is consolidated by the Cartesian product of the proposition of each uncertain variable. Therefore, the joint focal element of uncertain input of system response x_q^I is constructed and corresponding BBA of the joint belief structure are shown in equations (18) and (19):

$$x_q^\mathrm{I} = \left[\beta_{k_1}^\mathrm{I}, \mu_{\mathrm{u},k_2}^\mathrm{I}, \gamma_{k_3}^\mathrm{I}\right]^\mathrm{T} \quad k_1 \in \forall[1, K_1] \quad k_2 \in \forall[1, K_2] \quad k_3 \in \forall[1, K_3] \tag{18}$$

$$m_q = m_{k_1} \times m_{k_2} \times m_{k_3} \quad q \in \forall[1, Q] \quad Q = K_1 \times K_2 \times K_3 \tag{19}$$

in which, K_1, K_2 and K_3 are the number of focal element of β, μ_u and γ, respectively; Q is the number of joint focal element of system input. Due to the intervals that are used to

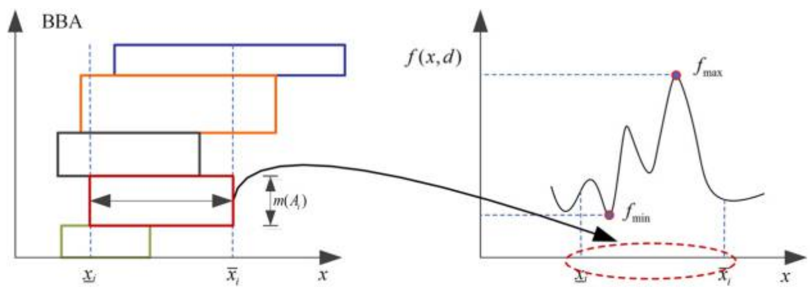

Figure 4.
Propagation of uncertainty

represent the uncertain parameters, the minimum and maximum responses of each x_q^I need to be found for closed spaces, as follows:

$$\left[\underline{R}_q, \overline{R}_q\right] = \left[\min R\left(x_q^{\mathrm{I}}\right), \max R\left(x_q^{\mathrm{I}}\right)\right] \qquad q \in \forall[1, Q] \tag{20}$$

where Q is the number of all possible joint belief structures. With the combination of the dimension of the variable vector and multiple intervals for each element of the vector, the uncertainty propagation involves an enormous joint hypercube and becomes very computationally unmanageable. To alleviate the computational cost, the differential evolution (DE) (Storn and Price, 1997) optimization approach is used for finding the propagated belief structure in this article.

As a novel evolutionary computational technique, DE was introduced by Storn and Price (1997) and has attracted much attention and seen wide application with a concise concept and easy implementation. From the perspective of the algorithm structure, DE seems to be a derivation of the traditional evolutionary algorithm (EA). Compared to traditional EAs, DE manifests its robust and fast convergence due to differences in the mutation scheme and selection process. Like other EAs, DE uses a D-dimensional parameter vector $\boldsymbol{x}_i = (x_{i1}, x_{i2}, \ldots, x_{iD})^{\mathrm{T}}$, $i = 1, 2, \ldots,$ NP to represent the trial solution of the objective function in each generation G ($G = 0, 1, 2, \ldots, G_{\max}$).

At the very beginning ($G = 0$), individuals in the NP population of the DE algorithm are generated as follows to cover the entire search space as much as possible:

$$x_{i,0}^j = x_{\min}^j + \mathrm{rand}(i) \times \left(x_{\max}^j - x_{\min}^j\right) \quad i = 1, 2, \ldots, \mathrm{NP} \quad j = 1, 2, \ldots, D \tag{21}$$

where $x_{\min}^j$ and $x_{\max}^j$ represent the minimum and maximum bounds of the jth candidate in each parameter vector. After the initial stage, like the EA family, mutation, crossover and selection are successfully used to improve the individual. At each generation G, the mutation method of DE/current-to-best/1/bin (Storn and Price, 1997) is used to add the competitor for each individual of the population:

$$\mathbf{v}_{i,G+1} = \mathbf{x}_{i,G} + F_1(\mathbf{x}_{\mathrm{best},G} - \mathbf{x}_{i,G}) + F_2(\mathbf{x}_{r1,G} - \mathbf{x}_{r2,G}) \tag{22}$$

where $\boldsymbol{x}_{\mathrm{best}}$ is the best individual of the population, F_1 and $F_2 > 0$ are real parameters, called mutation constants, and r_1 and r_2 are mutually different integers, randomly selected from the set $\{1, 2, \ldots, i-1, i+1, \ldots, \mathrm{NP}\}$. To increase the diversity of the population, a crossover operator is applied as:

$$u_{i,G+1}^j = \begin{cases} v_{i,G+1}^j & \mathrm{if}(\mathrm{rand}(j) \le CR)\ \mathrm{or}\left(j = \mathrm{randn}(i)\right) \\ x_{i,G+1}^j & \mathrm{if}(\mathrm{rand}(j) > CR)\ \mathrm{and}\left(j \ne \mathrm{randn}(i)\right) \end{cases} \tag{23}$$

where CR is a user defined crossover constant $\in [0, 1]$, $u_{i,G+1}^j$ is the component of the child that will compete with the parent, $x_{i,G+1}^j$, and $v_{i,G+1}^j$ are the new individuals, rand(j) is the jth independent random number uniformly distributed in the range of [0, 1], and randn(i) is a randomly chosen index from the set $\{1, 2, \ldots, D\}$. To keep the population size constant over subsequent generations, DE uses the following formulation to update its population:

$$\mathbf{x}_{G+1} = \begin{cases} \mathbf{u}_G & \text{if}\left(f(\mathbf{u}_G) < f(\mathbf{x}_G)\right) \\ \mathbf{x}_G & \text{otherwise} \end{cases} \tag{24}$$

where $\boldsymbol{x}_{G+1}$ is the updated individual, $\boldsymbol{x}_G$ is the old individual and $\boldsymbol{u}_G$ is the competitor. Thus, each competitor is compared with an old individual, and the better one passes to the next generation, so that the best individuals in the population are preserved. These steps are repeated until the specified termination criterion is reached. Meanwhile, the optimal results can be obtained. Then, the differential evolution global optimization method is used for propagation analysis of the represented uncertainty through the damage model.

3.3 Uncertainty measurement for performance-based seismic design

Once the process of uncertainty propagation is finished, the observed evidence of simulation responses is used to determine the target propositions for estimating uncertainty measures. As noted in above section, the belief (Bel) and plausibility (Pl) measures are used in evidence theory to express the uncertain measurement of proposition A:

$$\begin{aligned} \mathrm{Bel}(A) &= \sum\nolimits_{B \subseteq A} m(B) \\ \mathrm{Pl}(A) &= \sum\nolimits_{B \cap A \neq \varnothing} m(B) \end{aligned} \tag{25}$$

in which, B denotes distinct elements belonging to Θ and the belief function (Bel) and the plausibility function (Pl) are used to denote the degree of total belief and the degree of partial support of collection A using available evidence B, respectively. For the reason of epistemic uncertainty with the evocation of insufficient experimental data or inaccurate experience knowledge, the belief degree of event A cannot represent the confidence degree of $\tilde{A}$, that is $\mathrm{Bel}(A) + \mathrm{Bel}(\tilde{A}) \leq 1$. The expression of this relationship is shown in Figure 5.

In combination with the definition in equation (25), the $\mathrm{Bel}(L_R)$ and $\mathrm{Pl}(L_R)$ of proposition $L_R = \{R|\ R \in \boldsymbol{\Omega}, -\infty \leq R \leq R_{\mathrm{th}}\}$ are constructed as:

$$\mathrm{Bel}(L_R) = \sum\nolimits_{\overline{R}_q \leq R_{\mathrm{th}}} m_q \tag{26}$$

$$\mathrm{Pl}(L_R) = \sum\nolimits_{\underline{R}_q \leq R_{\mathrm{th}}} m_q \tag{27}$$

where R_{th} is the threshold value. The uncertain propagation results gives the minimum and maximum of system response $R_{\min}$ and $R_{\max}$ as following formula:

$$R_{\min} = \underset{q \in \forall[1,Q]}{\cup} \min\left(\underline{R}_q\right) \tag{28}$$

$$R_{\max} = \underset{q \in \forall[1,Q]}{\cup} \max\left(\overline{R}_q\right) \tag{29}$$

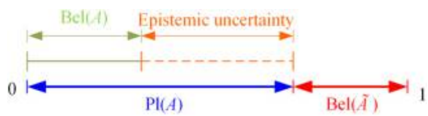

Figure 5.
Uncertainty description of proposition A

where $\underline{R}_q$ and $\overline{R}_q$ are represented the lower and upper system response of joint uncertain system input x_q^I. Given a series of $R_{th,\tau} \in \forall[R_{min}, R_{max}]$, the corresponding uncertain measures Bel ($R_{th,\tau}$) and Pl ($R_{th,\tau}$) constitute the cumulative belief function (CBF) and the cumulative plausibility function (CPF), respectively.

In the process of design, the risk level is designated, which means the design results shall be obtained under the specific confidence level. In consideration of the influence of epistemic uncertainty, the design result shall be determined by the specific confidence level of plausibility as following:

$$R_{th} = \mathrm{Pl}^{-1}(P_{th}) \tag{30}$$

where P_{th} denotes the threshold value of failure probability. According the formulation of equation (10), the yield force of ESDOF is obtained. Therefore, the seismic demand shear for each story of the structure is given by equations (31) and (32):

$$V_b = \Gamma_1^2 F_y \tag{31}$$

$$F_i = V_b \frac{G_i H_i}{\sum G_i H_i} \tag{32}$$

where V_b is the base shear of the building, F_i is the shear force for the ith floor, G_i is the weight of the ith floor and H_i is the height of the ith floor. Following these steps, a detailed elemental design for seismic capacity is implemented to determine the detailed information for each element. From above discussion, the flow chart of the UQ of PBSD is shown in Figure 6.

4. Case study

4.1 Details and preliminary design

To investigate the effectiveness of the proposed methods and the impact of the uncertain parameters on the Park–Ang damage model, we present the PBSD case for a six-story reinforced concrete frame that has regular distributions of mass and stiffness in plan and

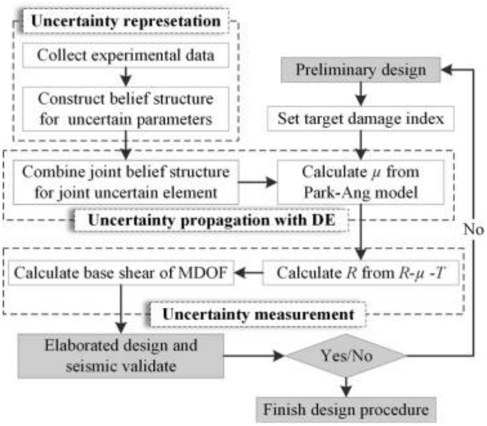

Figure 6. Flow chart of uncertainty quantification of PBSD

height. As shown in Figure 7, the height of each story is 3.6 m, while the other two principle directions, respectively, have two bays with a length of 5.7 m and six bays that are 4.2 m. The structure is located on a Grade III condition site (GB50011-2010, 2010). The location is classified as a degree VIII seismic fortification area with a 0.45 s design characteristic period of ground motion. The roof carries a dead load of 6.6 kN/m^2 and a floor live load of 1.0 kN/m^2, while other floors carry a dead load of 4.7 kN/m^2 and a live load of 2.0 kN/m^2. The design materials used in this example are C30 concrete and HRB400 rebar (GB50010-2010, 2010).

In the preliminary design, the cross-section geometries of all beams are empirically approximated as 250 × 650 mm and the cross-section are estimated as 600 × 600 mm and 550 × 550 mm for the columns in 1-3 and 4-6 story, respectively. Modal analysis affords the fundamental natural vibration period T_1 = 0.70 s, the value of the fundamental model participation parameter, $\Gamma_1 = 1.31$, and the value of $F_E = 9466$ kN. Under a rare earthquake, the reasonable strength reduction factor shall be determined through the threshold damage index that defaults to 0.9 (OU *et al.*, 1999). To investigate the influence of the uncertain parameters on the Park–Ang damage model for PBSD, we compare three different scenarios: an evidential model, a probabilistic model and a deterministic model.

4.2 Uncertainty quantification of performance-based seismic design analysis

To reduce the epistemic uncertainty of an input variable (n_0, k_p, ρ_w) and to estimate the reduction in uncertainty of the output (β), a sensitivity analysis based on a "pinching" strategy (Ferson and Troy Tucker, 2006) is adopted in this study. By comparing the uncertainty before and after "pinching" an input, i.e. replacing it with a scalar value without uncertainty, we can assess how much less uncertainty we would have if an input were available. The sensitivity index *SI* could be computed with the following expression:

$$SI = 100\left(1 - \text{unc(B)}/\text{unc(T)}\right)\% \tag{33}$$

where T is the baseline value of the expression, B is the value of the expression computed with an input pinched, and unc () is a measure of the uncertainty of the answer. Herein, we use the envelop area of CPF and CBF curves to denote the uncertainty measurement.

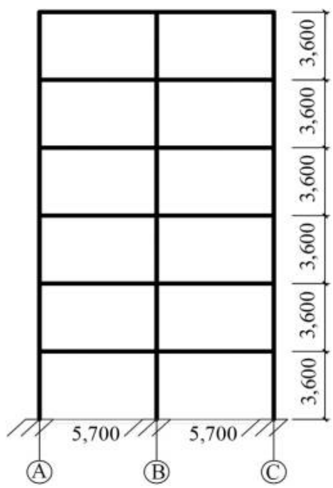

Figure 7.
Evaluation view of structure

Obviously, the narrower the envelope gets, the more influence the pinched variable has on the variability of the output. Using the uncertain information presented in Figure 1, the pinching sensitivity analysis results of β are shown in Figure 8.

In each subfigure (b, c and d) in Figure 8, the parameters n_0, k_p and ρ_w are separately pinched, while the others are varied in their belief structures. It is quite clearly visible that n_0 has a significant contribution to β with the biggest decrease of envelope area between CPF and CBF. However, the influence of the other two parameters k_p and ρ_w are negligible, producing 2.92 and 0.76 per cent reductions, respectively, of the envelope area between CPF and CBF. The results of these pinching analyses suggest that n_0 deserves focus in future empirical studies to reduce the overall epistemic uncertainty of β. For this case, the value of n_0 is approximated from preliminary design, and it ranges from 0.015 to 0.287. Based on the interval information of input uncertain parameter n_0, the histograms, interval relationships and belief structures based on data generated from the column database for model constant β are shown in Figure 9.

In accordance with a previous study (Rodriguez and Padilla, 2009), the variation of the ultimate ductility factor μ_u of a column is affected by the axial load ratio, shear-span ratio and volumetric transverse reinforcement ratio. Due to the lack of detailed information on the transverse reinforcement ratio, only the axial load ratio and the shear-span ratio are considered in the process of design. Typically, the shear-span ratio of frame columns can be considered as the ratio of column clear height and two times the maximum cross sectional dimension. Similarly, the uncertainty source of the dissipated factor is only dependent on the ultimate ductility factor because other factors are inaccessible in the structure design process. Finally, 11 components are selected to evaluate the values of μ_u and γ. The histograms, interval relationships and belief structures of these two parameters are shown in Figures 10 and 11.

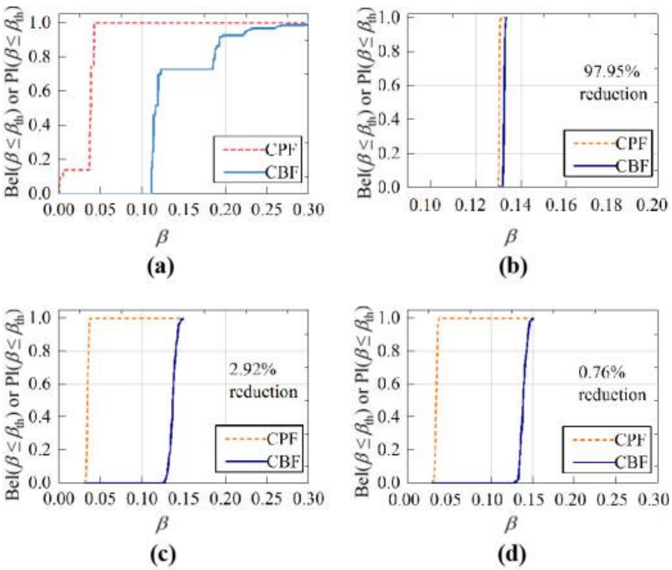

Notes: (a) n_0, k_p, and p_w are belief structures; (b) only n_0 pinched; (c) only k_p pinched; (d) only p_w pinched

Figure 8. Comparison of the sensitivity of parameter n_0, k_p and ρ_w for parameter β

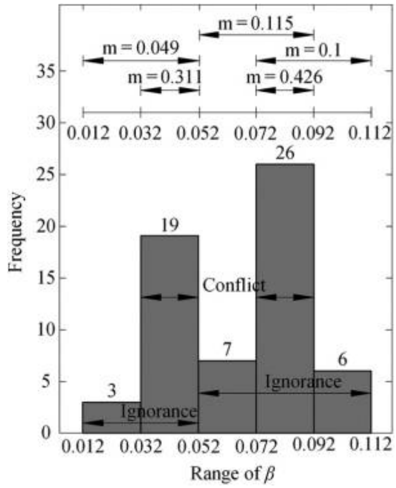

Figure 9. Histograms, interval relationships, and belief structures of β

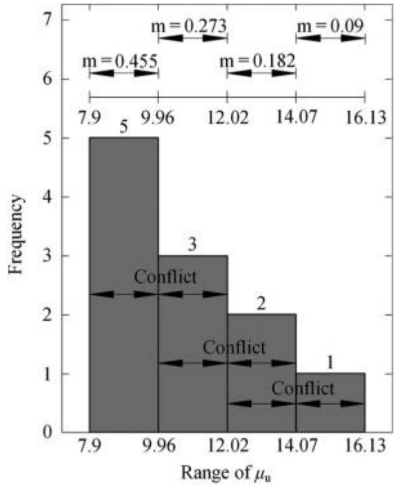

Figure 10. Histogram, interval relationship, and belief structure of μ_u

After the construction of evidential representation of three uncertain parameters, the DE interval optimal strategy is used to propagate the uncertainty response in each joint focal element. The initial population and the number iterations are set as 30 and 50, respectively. To validate the efficiency of DE-based interval propagation method, the brute force simulation is also used to propagate the epistemic uncertainties in Park–Ang model parameters. The samples of simulation in each joint focal element are set as10^4, 10^5 and 10^6, respectively. Figure 12 shows the UQ results of these four methods.

To illustrate the efficiency of DE-based interval optimal strategy with numerical comparison, Table II listed the CPF and CBF of R corresponding to the threshold probability $p = 0.05$.

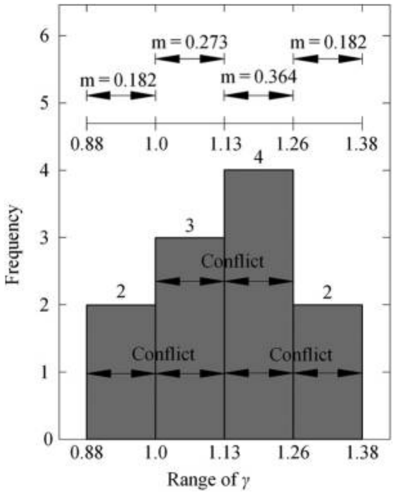

Figure 11. Histogram, interval relationship, and belief structure of γ

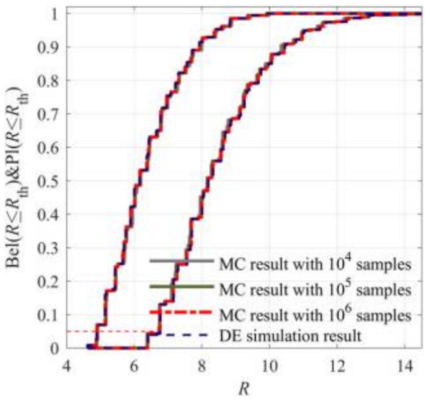

Figure 12. Comparison of belief and plausibility functions of R with MC and DE

Table II. Comparison of propagation results of R with MC simulations and DE

	MC with 10^4	MC with 10^5	MC with 10^6	DE
Lower bound	4.9173	4.8983	4.8920	*4.8860*
Upper bound	6.7221	6.7449	6.7534	*6.7721*

As shown in Table II, the accuracy of Monte-Carlo simulation improves by increasing the number of samples. However, it should be noted that the propagation results given by DE is more accuracy than Monte-Carlo simulation with 10^6 samples. According to the setup of DE algorithm, the number of computational process needs 1,500 times. That is to say that the DE interval optimal strategy obtained more robust result only needs 1,500 samples but the number of Monte-Carlo simulations costs 10^6 times. To illustrate the relationship of evidence theory and probability theory, an assumed probability theory distribution is constructed by supposing the parameters β, μ_u and γ satisfying the unified distributions in each bin of the histogram. Then, the probabilistic uncertainty propagation results is given as shown in Figure 13. For comparison, the uncertainty influences of Park–Ang model parameters, the results of a deterministic case with mean values of the design parameters β, μ_u and γ of 0.065, 10.76 and 1.13, respectively, are also given in Figure 13.

As manifested in Figure 13, the value of R corresponding to deterministic model is much smaller than the evidential and probabilistic model. In other words, the deterministic model may significantly underestimate the likelihood of a hypothetical unsafe region, and this will lead to an unsafe detailed design. However, the differences of the value of R between the evidential model and probabilistic model mainly derived from the level of completeness of collection data. The gap between the belief and plausibility values for a wide range of R values is indicative of the epistemic uncertainty embedded in the Park–Ang damage model. As for the cumulative distribution function (CDF) curve, the ordinate denotes the certain R probability. The CDF curve is located between the curves of CPF and CBF, which indicates that belief and plausibility are the lower and upper bounds of the R probability. This implies that probability is just a special case of evidence theory, and with the introduction of additional information or knowledge, the closed region of CPF and CBF is narrowed, and finally, the interval information is replaced by single points, and the evidence theory degenerates to probability.

Figure 13 also indicates that strategies for selecting reasonable intervals are used and effectively shrink the range for variable parameters the variability induced by the parametric uncertainty of the Park–Ang model is noticeable. To investigate the impact of uncertainty on the design results, the values of R with a 5 per cent of failure probability is selected. As shown in Figure 13, the gap between the upper bound and lower bound of evidential results is about 33.7 per cent of probabilistic result. This means the choice of target force reduction index R can fluctuate in [−12.8 per cent, 20.9 per cent] compare to the probabilistic result. To demonstrate the influence of the fluctuation of force reduction index R, Table III lists the worst case value of R corresponding to evidential model, probabilistic model and deterministic model. The yield resistant seismic force F_y and base shear V_b using the same threshold damage index $D = 0.9$ are also listed in Table III.

As shown in Table III, the R of an ESDOF corresponding to a 5 per cent confidence level of the plausibility of failure is 4.88. The 5 per cent confidence level of the probability of failure is 5.60, and the deterministic model result is 7.88. As the information is reflected in Figure 13 and Table III, the value of force reduction index R using evidential model and

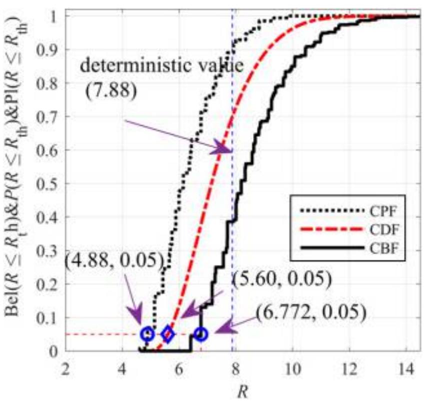

Figure 13. Comparison of cumulative belief, plausibility functions and cumulative distribution function of R

probabilistic model is much smaller than the deterministic model, which lead to larger base shear. The main reason for this difference because of the uncertainty rooted in Park–Ang model. As shown in Figure 13 and Table III, the difference between evidential model and probabilistic model can be seemed as the gap of one of realizations of epistemic uncertainty and the bounds of the most optimistic case and the worst case. In other words, the evidential results gives a more flexible design result compare to the fixed probabilistic result. Corresponding to the different choices for UQ models in Table III, detailed design results are listed in Table IV.

To investigate the seismic performance of RC frames with these three different models, a pushover analysis is carried out using the computation program OpenSees (Mazzoni *et al.*, 2006). The elements are modeled by the fiber-based nonlinear beam-column element. The confined and unconfined concrete fibers are characterized by the concrete 01 model, and the reinforcement fiber is modeled by steel 01. The pushover analysis is conducted by displacement control and ceased when the maximum inter-story drift exceeded 2 per cent, which is stipulated by the seismic code (GB50011-2010, 2010). The load pattern setting was an inverse triangle distribution, and the corresponding results are shown in Figure 14.

The detailed results of PBSD in Table III demonstrate a significant difference in reinforcement requirements between the uncertain and determined models. As expected, the validation results shown in Figure 14 also indicate different performances for the three models. The spectral accelerations of the worst case of evidential, probabilistic and deterministic models are decreased from 0.375 to 0.234 g. This means that on the condition of the same damage demand, the uncertain model would provide a more conservative design than the determined model. Compare to the validation result of worst case of evidential model and probabilistic model, it can be concluded that the flexibility of evidential model will give different performance choices for given damage demand. These situations also demonstrate that PBSD preferences are a set of trade-off solutions between robustness and uncertainty. From the perspective of robustness, the guarantee rate of the detailed design results for the deterministic model is far less than for consideration of uncertainty using

Result information	R_{design}	F_y(kN)	V_b(kN)
Evidence theory	4.88	1939	3348
Probability theory	5.60	1692	2921
Deterministic model	7.88	1201	2073

Table III. Comparison of the results of evidence, probability and deterministic models

	Results of evidential model				Results of probabilistic model				Results of deterministic model			
	Beams (mm^2)		Columns (mm^2)		Beams (mm^2)		Columns (mm^2)		Beams (mm^2)		Columns (mm^2)	
Story	Top	Bottom	Side	Middle	Top	Bottom	Side	Middle	Top	Bottom	Side	Middle
1	2235	1806	3246	2438	1916	1514	2404	1980	1345	986	1449	1350
2	2418	1938	1744	2303	2063	1621	1350	1881	1441	1052	1350	1350
3	2134	1697	1397	2242	1832	1426	1350	1852	1296	930	1350	1350
4	1652	1277	1363	2032	1437	1078	1134	1688	1040	706	1134	1134
5	1110	749	1134	1577	984	630	1134	1328	742	487	1134	1134
6	660	487	1134	1134	617	487	1134	1134	532	487	1134	1134

Table IV. Comparison of reinforcement area of evidential, probabilistic and deterministic model

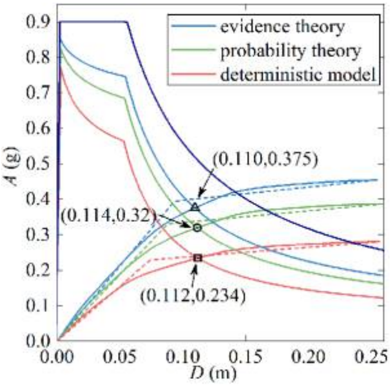

Figure 14.
Pushover analysis for three design models

probability theory and evidence theory. This implies that the deterministic elemental design results might be non-conservative. However, it should be noted that the results of the deterministic model will be more economical for sacrificing robustness.

The illustration in the case study shows that epistemic uncertainty in the design parameters of the Park–Ang damage model is inevitable, and while the Park–Ang damage index-based PBSD method is used routinely in seismic design activities, not much attention has been paid to this issue. Evidence theory has the general capability to handle epistemic uncertainty represented by discrete intervals or a continuous distribution and the powerful applicability of handling epistemic uncertainty without the additional assumptions that traditionally accompany classical probability theory.

5. Conclusion

In this article, an evidential uncertainty modeling method for the representation, propagation and quantification of uncertainty in Park–Ang damage models is developed. The parametric uncertainties in Park–Ang damage models are epistemic in nature and quantified in a non-probabilistic setting, which enables the designer to get free from the restrictions of classical probability theory, as well as alleviates the implicit assumptions of a complete data set. A differential evolution-based interval optimization technique is used to improve the computational efficiency in the evidence theory-based uncertainty propagation analysis. The application of the proposed approach was demonstrated on the UQ of the PBSD example for a six-story frame with consideration of a diverse set of experimental data from PEER. The experimental results show significant scatter of the Park–Ang model parameters, and the uncertainty in the damage model can have a significant influence on design results as expected. This implies that the existent deterministic analysis might be non-conservative. It might be worth noting that the epistemic uncertainty present in the Park–Ang damage model needs to be considered to avoid underestimating the true uncertainty.

References

Alarcón, E., Recuero, A., Perera, R., López, C., Gutiérrez, J.P., Diego, D.A., Picón, R. and Flórez-López, J. (2001), "A repairability index for reinforced concrete members based on fracture mechanics", *Engineering Structures*, Vol. 23 No. 6, pp. 687-697.

Azhdary, F. and Shabakhty, N. (2011), “Probabilistic evaluation of performance point in structures and investigation of the uncertainties”, *Journal of Mechanical Engineering Research*, Vol. 3 No. 6, pp. 197-208.

Bae, H.-R., Grandhi, R.V. and Canfield, R.A. (2004), “Epistemic uncertainty quantification techniques including evidence theory for large-scale structures”, *Computers and Structures*, Vol. 82 Nos 13/14, pp. 1101-1112.

Chopra, A.K. and Goel, R.K. (1999), *Capacity-Demand-Diagram Methods for Estimating Seismic Deformation of Inelastic Structures: SDF Systems*, PEER, University of CA, Berkeley, CA.

Datta, D. and Ghosh, S. (2008), “Uniform hazard spectra based on Park-Ang damage index”, *Journal of Earthquake and Tsunami*, Vol. 2 No. 3, pp. 241-258.

Dempster, A.P. (1967), “Upper and lower probabilities induced by a multivalued mapping”, *The Annals of Mathematical Statistics*, Vol. 38 No. 2, pp. 325-339.

Dubois, D. and Prade, H. (1988), *Possibility Theory: an Approach to Computerized Processing of Uncertainty*, Plenum press, New York, NY.

Fajfar, P. (1992), “Equivalent ductility factors, taking into account low-cycle fatigue”, *Earthquake Engineering and Structural Dynamics*, Vol. 21 No. 10, pp. 837-848.

FEMA356 (2000), “Prestandard and commentary for the seismic rehabilitation of buildings”, *FEMA-356*, Vol. 1, pp. 1-518.

Ferson, S. and Troy Tucker, W. (2006), “Sensitivity analysis using probability bounding”, *Reliability Engineering and System Safety*, Vol. 91 Nos 10/11, pp. 1435-1442.

FIP (2003), *Displacement-Based Seismic Design of Reinforced Concrete Buildings*, The International Federation for Structural Concrete, Lausanne, Switzerland.

GB50010-2010 (2010), “Code for the design of concrete structures”.

GB50011-2010 (2010), “Code for seismic design of buildings”.

Ghosh, S. and Collins, K.R. (2006), “Merging energy-based design criteria and reliability-based methods: exploring a new concept”, *Earthquake Engineering and Structural Dynamics*, Vol. 35 No. 13, pp. 1677-1698, available at: internal-pdf://110.56.253.131/Mergingenergy-baseddesigncriteriaandrelia.pdf

Ghosh, S., Datta, D. and Katakdhond, A.A. (2011), “Estimation of the Park–Ang damage index for planar multi-storey frames using equivalent single-degree systems”, *Engineering Structures*, Vol. 33 No. 9, pp. 2509-2524.

Hajirasouliha, I., Asadi, P. and Pilakoutas, K. (2012), “An efficient performance-based seismic design method for reinforced concrete frames”, *Earthquake Engineering and Structural Dynamics*, Vol. 41 No. 4, pp. 663-679.

Helton, J.C. (1997), “Uncertainty and sensitivity analysis in the presence of stochastic and subjective uncertainty”, *Journal of Statistical Computation and Simulation*, Vol. 57 Nos 1/4, pp. 3-76.

Jiang, H., Lu, X. and Kubo, T. (2010), “Damage displacement estimation of flexure-dominant RC columns”, *Advances in Structural Engineering*, Vol. 13 No. 2, pp. 357-368.

Karbassi, A., Mohebi, B., Rezaee, S. and Lestuzzi, P. (2014), “Damage prediction for regular reinforced concrete buildings using the decision tree algorithm”, *Computers and Structures*, Vol. 130, pp. 46-56.

Klir, G.J. and Smith, R.M. (2001), “On measuring uncertainty and uncertainty-based information: recent developments”, *Annals of Mathematics and Artificial Intelligence*, Vol. 32 Nos 1/4, pp. 5-33.

Kunnath, S., Reinhorn, A. and Park, Y. (1990), “Analytical modeling of inelastic seismic response of R/C structures”, *Journal of Structural Engineering*, Vol. 116 No. 4, pp. 996-1017.

Lo, C.-K., Pedroni, N. and Zio, E. (2014), “Treating uncertainties in a nuclear seismic probabilitistic risk assessment by means of the dempster-shafer theory”, *Nuclear Engineering and Technology*, Vol. 46 No. 1, pp. 11-26.

Mazzoni, S., McKenna, F., Scott, M.H. and Fenves, G.L. (2006), *Open System for Earthquake Engineering Simulation (OpenSees)*, PEER, University of CA, Berkeley.

Miranda, E. (1993), "Site-dependent strength-reduction factors", *Journal of Structural Engineering*, Vol. 119 No. 12, pp. 3503-3519.

Moore, R.E. (1966), *Interval Analysis*, Prentice-Hall, Englewood Cliffs.

Oberkampf, W.L., Helton, J.C. and Sentz, K. (2001), "Mathematical representation of uncertainty", in *American Institute of Aeronautics and Astronautics Non-Deterministic Approaches Forum*, American Institute of Aeronautics and Astronautics Non-Deterministic Approaches Forum, *Seattle, WA*, pp. 1-23.

Ou, J.P., He, Z., Wu, B. and Qiu, F.W. (1999), "Seismic damage performance-based design of reinforced concrete structures", *Earthquake Engineering and Engineering Vibration*, Vol. 19 No. 1, pp. 21-30.

Panagiotakos, T.B. and Fardis, M.N. (2001), "Deformations of reinforced concrete members at yielding and ultimate", *ACI Structural Journal*, Vol. 98 No. 2, pp. 135-148.

Park, R. (1988), "Ductility evaluation from laboratory and analytical testing", in *Proceedings of the 9th World Conference on Earthquake Engineering, Tokyo-Kyoto, Japan*, pp. 605-616.

Park, Y.J. and Ang, A.H.S. (1985), "Mechanistic seismic damage model for reinforced concrete", *Journal of Structural Engineering*, Vol. 111 No. 4, pp. 722-739.

Park, Y.-J., Ang, A.-S. and Wen, Y.-K. (1984), *Seismic Damage Analysis and Aamage-Limiting Design of RC Buildings*, University of Illinois Engineering Experiment Station, College of Engineering, University of Illinois at Urbana-Champaign, Champaign, IL.

Park, Y.-J., Ang, A.H.S. and Wen, Y.K. (1985), "Seismic damage analysis of reinforced concrete buildings", *Journal of Structural Engineering*, Vol. 111 No. 4, pp. 740-757.

Park, Y.J., Ang, A.H. and Wen, Y.K. (1987), "Damage-limiting aseismic design of buildings", *Earthquake Spectra*, Vol. 3 No. 1, pp. 1-26.

Priestley, M.J.N., Calvi, G.M. and Kowalsky, M.J. (2007), "Direct displacement-based seismic design of structures", in *5th NZSEE Conference*.

Rajabi, R., Barghi, M. and Rajabi, R. (2013), "Investigation of Park–Ang damage index model for flexural behavior of reinforced concrete columns", *The Structural Design of Tall and Special Buildings*, Vol. 22 No. 17, pp. 1350-1358.

Rodriguez, M.E. and Padilla, D. (2009), "A damage index for the seismic analysis of reinforced concrete members", *Journal of Earthquake Engineering*, Vol. 13 No. 3, pp. 364-383.

Salehghaffari, S., Rais-Rohani, M., Marin, E.B. and Bammann, D.J. (2012), "A new approach for determination of material constants of internal state variable based plasticity models and their uncertainty quantification", *Computational Materials Science*, Vol. 55, pp. 237-244.

Sallak, M., Schön, W. and Aguirre, F. (2013), "Reliability assessment for multi-state systems under uncertainties based on the Dempster–Shafer theory", *IIE Transactions*, Vol. 45 No. 9, pp. 995-1007.

SEAOC Vision 2000 (1995), *Performance-Based Seismic Engineering*, Structural Engineers Association of CA, Sacramento, CA.

Shafer, G. (1976), *A Mathematical Theory of Evidence*, Princeton university press Princeton, Princeton.

Storn, R. and Price, K. (1997), "Differential evolution – a simple and efficient heuristic for global optimization over continuous spaces", *Journal of Global Optimization*, Vol. 11 No. 4, pp. 341-359.

Tang, H., Su, Y. and Wang, J. (2015), "Evidence theory and differential evolution based uncertainty quantification for buckling load of semi-rigid jointed frames", *Sadhana*, Vol. 40 No. 5, pp. 1611-1627.

University of Washington (2004), "The UW-PEER reinforced concrete column test database".

Vidic, T., Fajfar, P. and Fischinger, M. (1994), "Consistent inelastic design spectra – strength and displacement", *Earthquake Engineering and Structural Dynamics*, Vol. 23 No. 5, pp. 507-521.

Walley, P. (1991), *Statistical Reasoning with Imprecise Probabilities*, Chapman and Hall, London.

Williams, M.S. and Sexsmith, R.G. (1997), "Seismic assessment of concrete bridges using inelastic damage analysis", *Engineering Structures*, Vol. 19 No. 3, pp. 208-216.

Zadeh, L.A. (1965), "Fuzzy sets", *Information and Control*, Vol. 8 No. 3, pp. 338-353.

Zhai, C.H., Wen, W.P., Zhu, T.T., Li, S. and Xie, L.L. (2013), "Inelastic displacement ratios for design of structures with constant damage performance", *Engineering Structures*, Vol. 52, pp. 53-63.

Zhang, Y.L., Jiang, J.Q., Liu, J.J. and Wang, Z.Y. (2011), "Seismic damage assessment of reinforced concrete structure and its seismic design", *Journal of Zhejiang University (Engineering Science)*, Vol. 7, p. 27.

Zhuo, W. and Fan, L. (2001), "On strength reduction factors used for seismic design of structures", *Earthquake Engineering and Engineering Vibration*, Vol. 21 No. 1, pp. 84-88.

Corresponding author
Hesheng Tang can be contacted at: thstj@tongji.edu.cn